

# Particle number fluctuations in a membrane channel

Sergey M. Bezrukov<sup>a)</sup>

*Laboratory of Physical and Structural Biology, NICHD, National Institutes of Health, Bethesda, Maryland 20892 and St. Petersburg Nuclear Physics Institute, Gatchina, 188350 Russia*

Alexander M. Berezhkovskii

*Laboratory of Physical and Structural Biology, NICHD, National Institutes of Health, Bethesda, Maryland 20892 and Karpov Institute of Physical Chemistry, Vorontsovo Pole 10, Moscow, K-64, 103064 Russia*

Mark A. Pustovoit

*St. Petersburg Nuclear Physics Institute, Gatchina, 188350 Russia*

Attila Szabo

*Laboratory of Chemical Physics, NIDDK, National Institutes of Health, Bethesda, Maryland 20892*

(Received 2 May 2000; accepted 14 August 2000)

Channel-facilitated transport of metabolites across biological membranes results in excess noise in the current carried by small ions. This noise originates from fluctuations of the number of metabolite molecules in the channel due to their diffusion. We have carried out a theoretical study of particle number fluctuations in a cylindrical pore. First, we obtain the power spectral density of these fluctuations as a function of pore length and radius, as well as the diffusion constants of the particle in the pore and in the bulk, in the absence of particle–pore interactions. We then perform three-dimensional Brownian dynamics simulations that show excellent agreement with the analytical result. Finally, we demonstrate that explicit expressions for the low-frequency limit of the spectral density can be found even when the particle interacts with the pore. © 2000 American Institute of Physics. [S0021-9606(00)70842-7]

## I. INTRODUCTION

In this paper we analyze fluctuations of the number of diffusing particles in a cylindrical channel connecting two reservoirs shown in Fig. 1. This problem arises in connection with the measurements of the diffusion constants of metabolites inside membrane channels. It is now firmly established that transport of metabolites and, more generally, high-molecular-weight solutes occurs through large channels in the cell membranes.<sup>1</sup> Examples of such channels include bacterial porins, mitochondrial channels, gap junctions, the nuclear pore complex, and protein-conducting channels in the endoplasmic reticulum. A recent study<sup>2</sup> even suggests that particles as large as phage f1 (about 7 nm in diameter) can exit host cells with the help of a phage-encoded channel protein.

The membrane transport properties for solutes other than monoatomic ions are usually determined from macroscopic fluxes of the molecules in question through multichannel objects such as cells, cell organelles, or liposomes. The macroscopic flux measurements involve radioactive, fluorescent, or colorimetric probes,<sup>3</sup> electron-opaque tracers,<sup>4</sup> liposome swelling,<sup>5</sup> or solute-specific reactions, such as the luciferin–luciferase system for adenosine triphosphate detection.<sup>6</sup>

Alternatively, the transport properties can be determined by measuring how the addition of metabolite influences the

electrolyte ion current through the membrane channel. The current decreases when a neutral metabolite molecule enters the channel. The average decrease of the current is proportional to the average number of molecules inside the channel when this number is small. From solute-induced current fluctuations measured with the time resolution of a typical single-channel experiment (usually in the range of tens or hundreds of micro-seconds), it is possible to deduce diffusion constant corresponding to the much faster transients (e.g., in the nanosecond range).<sup>7</sup>

One can characterize solute-induced fluctuations in the ion current  $i$  in terms of the experimentally accessible parameter—the power spectral density,  $S_i(f)$ . In situations where the average number of metabolite molecules in the channel,  $\langle N \rangle$ , is small enough to neglect interactions between molecules,  $S_i(f)$  is proportional to the normalized power spectral density of molecule number fluctuations,  $S(f)$ ,

$$S_i(f) = \langle N \rangle (\Delta g)^2 V^2 S(f), \quad (1)$$

where  $\Delta g$  is the reduction in channel conductance upon entering of one metabolite molecule,  $V$  is the applied voltage.<sup>7</sup> The spectral density can be expressed in terms of the normalized correlation function of the number of metabolites in the channel,  $C(t)$  (e.g., see Ref. 8)

$$S(f) = 4 \int_0^\infty C(t) \cos(2\pi ft) dt. \quad (2)$$

<sup>a)</sup> Author to whom correspondence should be addressed. Telephone: (301) 402-4701; Fax: (301) 402-9462. Electronic mail: bezrukov@helix.nih.gov

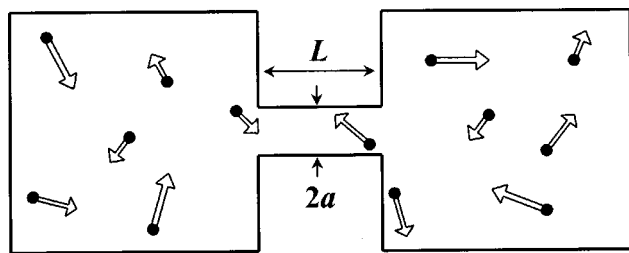


FIG. 1. A cylindrical channel of length  $L$  and radius  $a$  in equilibrium with two reservoirs. Due to diffusion, Brownian particles exchange between the channel and the bulk. Arrows illustrate random displacement of particles during time increment  $\Delta t$ . The instantaneous particle number in the channel fluctuates (see Fig. 3), giving rise to channel conductance fluctuations.

This expression shows that the spectral density is the Fourier transform of the number correlation function. The correlation function is identical to the probability of finding a particle in the channel given that initially the particle was uniformly distributed in the channel (that is, the survival probability of the particle).

Conductance noise arising from the stochastic nature of matter (or heat) exchange between the sample and the “bath” has been repeatedly addressed for at least half a century.<sup>9</sup> In some cases, for example, for the uniform three-dimensional diffusion of particles in and out of a spherical volume,<sup>10</sup> exact expressions for the power spectral density of the particle number fluctuations have been obtained. However, for a cylindrical channel connecting two reservoirs this is not the case. To estimate the low-frequency components and frequency width of the particle number fluctuations inside the channel, different groups use different expressions relating these quantities to the channel length,  $L$ , and diffusion constant inside the channel,  $D$ . For example, the frequency width has been estimated as  $D/\pi L^2$  (Ref. 11),  $D/L^2$  (Ref. 12), or  $6D/\pi L^2$  (this estimate follows from the characteristic diffusion relaxation time,  $L^2/12D$ , given by Feher and Weissman<sup>13</sup> and by Berg,<sup>14</sup> if one assumes a simple Lorentzian shape for the noise spectrum). Though all these expressions indeed retain the  $D/L^2$  ratio, they give different numerical factors for the cut-off frequency and, therefore, for the low-frequency spectral density. Moreover, all these expressions, being independent of the channel radius,  $a$ , in fact, are obtained for a long and narrow channel for which  $L/a \gg 1$  and, therefore, one can neglect the particle return probability.

In this paper we obtain the Fourier transform of the number correlation function by reducing the three-dimensional problem to the effective one-dimensional problem for the particle diffusing in the channel. We obtain an analytical expression for the spectral density as a function of frequency, which depends on the length and radius of the channel as well as the diffusion constants of the particle in the channel and in the bulk. The analytical result is in excellent agreement with the spectral density found by Brownian dynamics simulations. Finally, we show how one can analytically obtain the low-frequency limit of the spectral density for the case of arbitrary potential  $U(x)$  along the channel as well as arbitrary dependence of the diffusion coefficient on particle's position inside the channel.

It is worth mentioning that often there is a highly specific binding site for the metabolite inside the channel pore. One of the well known examples is sugar interaction with the maltoporin channel.<sup>15,16</sup> If the mean lifetime of the metabolite on the site is comparable or larger than  $L^2/D$ , the noise spectral density can be dramatically different from the one discussed here and will be considered in a forthcoming publication.

## II. STATEMENT OF THE PROBLEM

Consider two compartments connected by a cylindrical channel of radius  $a$  and length  $L$  (Fig. 1) containing noninteracting particles that diffuse independently. The diffusion constants in the channel and in the bulk will be denoted by  $D$  and  $D_b$ , respectively. We will find the normalized correlation function of the number of particles in the channel by calculating the time-dependent probability of finding a particle in the channel given that initially the particle was uniformly distributed along the channel.

It is natural to approximate the motion in the channel as one-dimensional. The probability density  $p(x,t)=p$  inside the channel satisfies the equation

$$\frac{\partial p}{\partial t} = D \frac{\partial^2 p}{\partial x^2}, \quad 0 < x < L, \quad (3)$$

and the initial condition  $p(x,0)=1/L$ . This equation must be supplemented by boundary conditions at  $x=0,L$ , which will be discussed below. The correlation function of interest is the survival probability and is given by

$$C(t) = \int_0^L p(x,t) dx. \quad (4)$$

We will solve Eq. (3) by the Laplace transform method. Given the Laplace transform of the survival probability

$$\hat{C}(s) = \int_0^\infty e^{-st} C(t) dt, \quad (5)$$

one can find the spectral density by the relation

$$S(f) = 4 \operatorname{Re} \{ \hat{C}(s = i2\pi f) \}. \quad (6)$$

Thus, the calculation of  $S(f)$  reduces to finding the Laplace transform of the survival probability.

## III. ANALYTIC EXPRESSION FOR THE SPECTRAL DENSITY

The formalism of this section is based on boundary conditions that are obtained using intuitive arguments. In the next section, using a more rigorous approach, we will show that the analytic expression for the spectral density obtained below is valid except at very high frequencies ( $fa^2/D \gg 1$ ).

A particle reaching the channel end may escape to infinity or may return back into the channel. To describe this we use radiation boundary conditions of the form

$$D \frac{\partial p(x,t)}{\partial x} \Big|_{x=0} = \kappa p(0,t); \quad D \frac{\partial p(x,t)}{\partial x} \Big|_{x=L} = -\kappa p(L,t), \quad (7)$$

where  $\kappa$  is a rate constant characterizing the “efficiency of escape” at the endpoints.

To find  $\kappa$  we consider a particle in a system of two compartments connected by a channel (Fig. 1) at equilibrium. It is equally probable to find the particle at any point and, therefore, the equilibrium density is a constant,  $p_{\text{eq}} = 1/V$ , where  $V$  is the total volume of the system. The effective one-dimensional density inside the channel is also constant and given by  $p_{1-d\text{eq}} = \pi a^2/V$ . We determine  $\kappa$  from the condition that fluxes entering and leaving the channel are equal to each other. The flux escaping the channel into a compartment is  $j_{\text{out}} = \kappa \pi a^2/V$ . This flux is compensated by the entering flux,  $j_{\text{in}} = 4D_b a/V$ , where the rate constant,  $4D_b a$ , describes the steady-state trapping of particles by an absorbing disk of radius  $a$  located on a reflecting wall.<sup>17</sup> Since  $j_{\text{in}} = j_{\text{out}}$ , we obtain

$$\kappa = \frac{4D_b}{\pi a}. \quad (8)$$

This rate constant depends on the bulk diffusion constant. When  $D_b \rightarrow \infty$  or  $a \rightarrow 0$ ,  $\kappa \rightarrow \infty$  which means that the endpoints become perfectly absorbing.

To find the survival probability one has to solve the diffusion equation [Eq. (3)] with the boundary conditions in Eq. (7) and the initial condition  $p(x,0) = 1/L$ . Laplace transforming Eq. (3) we have

$$S(f) = \frac{1}{\pi f \alpha} \frac{2\beta(\sinh^2 \alpha + \sin^2 \alpha) + \sinh(2\alpha) - \sin(2\alpha)}{2(\sinh^2 \alpha + \cos^2 \alpha) + \beta(\sinh(2\alpha) - \sin(2\alpha)) + \beta^2(\sinh^2 \alpha + \sin^2 \alpha)}, \quad (12)$$

where

$$\alpha = \sqrt{\frac{\pi f}{D}} \frac{L}{2}; \quad \beta = \frac{4D}{L\kappa} \alpha = \frac{\pi a D}{L D_b} \alpha = \sqrt{\frac{\pi^3}{4}} \frac{a^2 D}{D_b^2} f. \quad (13)$$

By putting  $\beta=0$  we find  $S_a(f)$  corresponding to perfectly absorbing endpoints

$$S_a(f) = \frac{\sqrt{D}}{(\pi f)^{3/2} L} \frac{\sinh\left(\sqrt{\frac{\pi f}{D}} L\right) - \sin\left(\sqrt{\frac{\pi f}{D}} L\right)}{\sinh^2\left(\sqrt{\frac{\pi f}{D}} \frac{L}{2}\right) + \cos^2\left(\sqrt{\frac{\pi f}{D}} \frac{L}{2}\right)}. \quad (14)$$

The expression for  $S(f)$  takes into account the finiteness of the ratio  $a/L$  while  $S_a(f)$  corresponds to the limiting case when the ratio is zero. The most interesting qualitative manifestation of the finiteness of this ratio is the increase of the low-frequency “white” part of the spectrum,  $S(0)$ , compared to  $S_a(0)$

$$S(0) = S_a(0) \left(1 + \frac{3\pi}{2} \frac{D a}{D_b L}\right), \quad S_a(0) = \frac{L^2}{3D}. \quad (15)$$

$$s\hat{p} - \frac{1}{L} = D \frac{\partial^2 \hat{p}}{\partial x^2}. \quad (9)$$

The solution of this equation satisfying the initial and boundary conditions is

$$\hat{p}(x,s) = \frac{1}{Ls} \left[ 1 - \frac{\kappa \cosh\left(\sqrt{\frac{s}{D}} \left(x - \frac{L}{2}\right)\right)}{\kappa \cosh\left(\sqrt{\frac{s}{D}} \frac{L}{2}\right) + \sqrt{sD} \sinh\left(\sqrt{\frac{s}{D}} \frac{L}{2}\right)} \right]. \quad (10)$$

Integrating this with respect to  $x$  over the interval  $(0,L)$ , we find the Laplace transform of the survival probability

$$\hat{C}(s) = \frac{1}{s} - \frac{1}{s \left[ s \frac{L}{2\kappa} + \sqrt{\frac{s}{D}} \frac{L}{2} \coth\left(\sqrt{\frac{s}{D}} \frac{L}{2}\right) \right]}. \quad (11)$$

Using Eq. (6) we find

The expression for  $S_a(0)$  was obtained earlier.<sup>18</sup> It is seen that the second term in parentheses disappears if  $D/D_b$  and/or  $a/L$  approach zero. For comparison, in Fig. 2 we draw  $S(f)$  and  $S_a(f)$  for  $a/L = 0.025, 0.05$ , and  $0.25$  taking  $D = D_b$ .

To estimate the level of accuracy of the analytical result obtained above we performed Brownian dynamics simulations of the system in Fig. 1. A typical time record of the number of particles in the channel is presented in Fig. 3. It gives a small fragment of the total trajectory that was used to calculate the spectral density. The particle number fluctuates between zero, one, two, and, rarely, three (the central part of the upper trace). The events corresponding to a particle's passage *through* the channel are marked by the pairs of upward and downward arrows. These events are relatively long. An upward arrow shows the moment a particle enters the channel; the following downward arrow shows the moment this particle escapes from the *opposite* side of the channel. It is seen that most of the events are unmarked. They correspond to realizations when particles enter and leave the channel from the same side. These events are obviously much shorter than those corresponding to the particle translocations through the channel.

The particle number correlation function and spectral density can be calculated from long trajectories of this type.

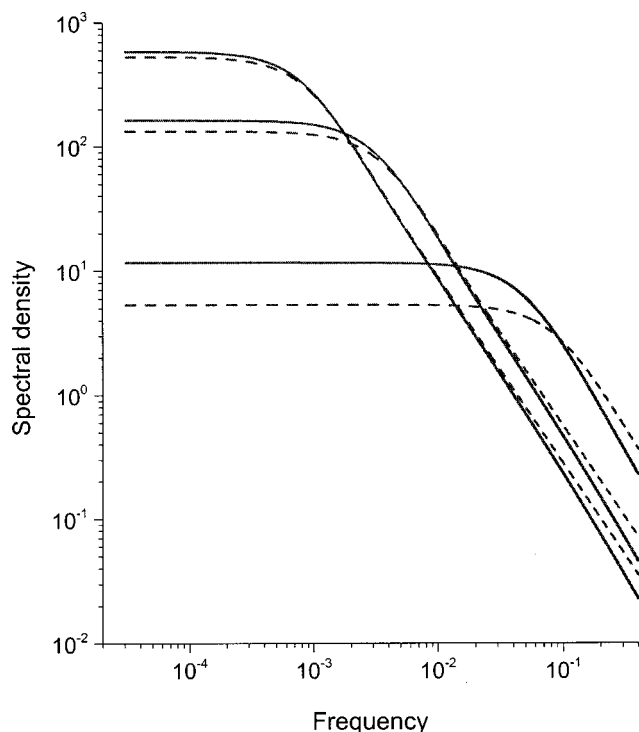


FIG. 2. Theoretical predictions for  $S(f)$  (solid lines) and  $S_a(f)$  (dashed lines), Eqs. (12) and (14), compared for channels with different  $a/L$  ratios at  $a=1$ , and  $D_b=D=1$ . From top to bottom:  $a/L=0.025, 0.05$ , and  $0.25$ . It is seen that as the channel length decreases, the bends of the spectral curves move to the right, to higher frequencies. Simultaneously, the curves move downward to preserve the area under the curve which is normalized to one. This normalization can be checked using Eq. (2).

Figure 4 compares the spectral density obtained from Eq. (12) with simulation results. Good agreement is found not only for long channels (e.g., the top trace,  $L/a=40$ ), but also for relatively short ones (e.g., the bottom trace,  $L/a=4$ ). Equation (12) adequately describes both the low-frequency, white part of the power spectrum and its high-frequency tail.<sup>19</sup>

#### IV. A MORE SOPHISTICATED SOLUTION OF THE PROBLEM

The solution obtained above is based on using the radiation boundary conditions, Eq. (7), with  $\kappa$  given by Eq. (8). Now we will derive boundary conditions in a more rigorous way in order to rationalize the excellent agreement between such a simple theory and simulations. This can be done by matching the solution inside the channel with the bulk solution outside the channel.

In the bulk, outside the channel, the problem is three-dimensional and the probability density,  $p_3(\rho, x, t) = p_3$ , satisfies the equation (we now use cylindrical coordinates with  $\rho$  denoting the distance from the channel axis)

$$\frac{\partial p_3}{\partial t} = D_b \nabla^2 p_3, \quad x < 0, \quad x > L. \quad (16)$$

Inside the channel the problem is also three-dimensional. However, it can be reduced to a one-dimensional problem if (a) the initial concentration is uniform and (b) it is as-

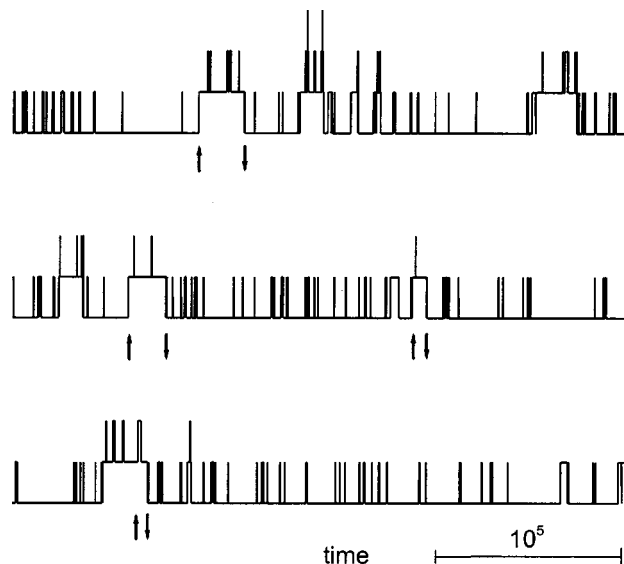


FIG. 3. Number of particles in the channel as a function of time obtained in numerical simulations. Three-dimensional Brownian trajectories were generated using three normally distributed random variables that determined the jump of a particle in each direction during the discrete time step  $\Delta t$ . The values of parameters were chosen so that  $2D\Delta t \ll a^2$ , making the diffusion simulation effectively continuous in space. Collisions with the walls were assumed to be elastic. The reservoir size was taken to be much larger than the channel diameter  $a$  (namely,  $50 \times 50 \times 50$  for  $a=1$ ) to get rid of finite size effects. The traces presented here have been obtained for  $L=20$ ,  $D=5 \cdot 10^{-3}$  with the total of 640 particles in the system. A time interval corresponding to  $10^5$  time steps is shown below the record.

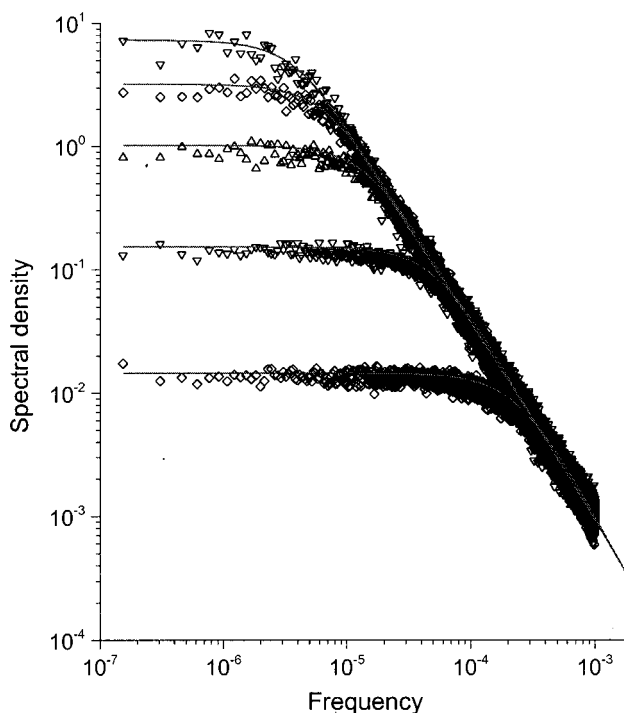


FIG. 4. Spectral density obtained from numerical simulations in comparison with the theoretical predictions. Solid lines are drawn according to Eq. (1) with  $\langle N \rangle = L\pi a^2 n$  and  $S(f)$  given in Eq. (12). Parameters are: particle concentration  $n=0.01$ ,  $\Delta g=0.1$ ,  $a=V=1$ ,  $D_b=D=5 \cdot 10^{-3}$ , and  $L=40; 30; 20; 10; 4$ , from top to bottom. Excellent agreement between the theory and the simulations is seen over the entire frequency range.



sumed that the cross-sectional concentration profile at the ends of the channel remains uniform for all time. After these assumptions have been made, this problem can be solved exactly.

The probability density for the one-dimensional problem satisfies Eq. (3). To match the intrachannel and bulk solutions, we use the continuity of the probability density and the flux at the channel boundary. This leads to (we consider only the left boundary located at  $x=0$ )

$$p(0,t) = \pi a^2 p_3(\rho,0,t), \quad 0 < \rho < a \quad (17)$$

and

$$D \frac{\partial p(x,t)}{\partial x} \Big|_{x=0} = 2\pi D_b \int_0^a \rho \frac{\partial p_3(\rho,x,t)}{\partial x} \Big|_{x=0} d\rho. \quad (18)$$

The probability density  $p_3(\rho,x,t)$  can be expressed in terms of the concentration that arises in calculating the flux into the absorbing disk. The disk has radius  $a$  and is located on a reflecting wall at  $x=0$ , so that its center is at the origin,  $\rho=x=0$ . The concentration  $c(\rho,x,t)$  satisfies the equation

$$\frac{\partial c}{\partial t} = D_b \nabla^2 c, \quad x < 0, \quad (19)$$

with the boundary conditions

$$c(\rho,0,t)|_{\rho < a} = 0, \quad \frac{\partial c(\rho,x,t)}{\partial x} \Big|_{x=0, \rho > a} = 0, \quad (20)$$

and the initial condition  $c(\rho,x,0) = 1$ . Time-dependent rate coefficient describing the trapping is given by

$$k(t) = 2\pi D_b \int_0^a \rho \left[ -\frac{\partial c(\rho,x,t)}{\partial x} \Big|_{x=0} \right] d\rho. \quad (21)$$

The infinite time limit of  $k(t)$  is  $4D_b a$ , the quantity used to determine  $\kappa$  in Eq. (8).

It is most convenient to give the relation between  $p_3$  and  $c$  in Laplace domain. The relation is

$$\hat{p}_3(\rho,x,s) = \frac{1}{\pi a^2} \hat{p}(0,s) [1 - s \hat{c}(\rho,x,s)]. \quad (22)$$

One can check that this  $p_3(\rho,x,s)$  satisfies the Laplace transform of the diffusion equation in Eq. (16), the reflecting boundary conditions on the wall, and the matching condition in Eq. (17). After substituting this result into the Laplace transform of the second matching condition in Eq. (18), we obtain

$$D \frac{\partial \hat{p}(x,s)}{\partial x} \Big|_{x=0} = \frac{s \hat{k}(s)}{\pi a^2} \hat{p}(0,s), \quad (23)$$

where  $\hat{k}(s)$  is the Laplace transform of  $k(t)$ .

Equation (23) provides the boundary condition at  $x=0$  for the effectively one-dimensional problem inside the channel. In the same way one can derive the boundary condition at  $x=L$

$$D \frac{\partial \hat{p}(x,s)}{\partial x} \Big|_{x=L} = -\frac{s \hat{k}(s)}{\pi a^2} \hat{p}(L,s) \quad (24)$$

Solving the one-dimensional problem with the boundary conditions in Eqs. (23) and (24) it can be shown that the Laplace transform of the survival probability,  $\hat{C}(s)$ , is given by the expression in Eq. (11) with  $\kappa$  replaced by  $s \hat{k}(s)/\pi a^2$ . This result is exact for the problem specified by Eqs. (16)–(18).

To compare the boundary conditions in Eqs. (23) and (24) with those given in Eq. (7), we use the approximate expression for  $\hat{k}(s)$  (Ref. 20)

$$\hat{k}(s) = \frac{4aD_b}{s} \left[ 1 + \frac{\pi}{4} \sqrt{\frac{sa^2}{D_b}} \left( 1 - \frac{\frac{4}{\pi} - 1}{\frac{\pi(4-\pi)}{\pi^2-8} + \sqrt{\frac{sa^2}{D_b}}} \right) \right]. \quad (25)$$

This expression reproduces the first two terms in both large- $s$  and small- $s$  expansions of the rate constant. The corresponding expression in time domain is exact at short and long times; at intermediate times it is within one percent of the results of numerical solution of the diffusion equation. Equation (25) shows that  $s \hat{k}(s)$  approaches  $4aD_b$  when  $s < D_b/a^2$ . In time domain this means that  $k(t)$  approaches its plateau value  $4aD_b$  on times of the order of  $a^2/D_b$ . Thus, on times larger than  $a^2/D_b$ , the boundary conditions in Eq. (7) and Eqs. (23) and (24) coincide.

Finally, we note that the boundary condition in Eq. (24) in time domain has the form

$$D \frac{\partial p(x,t)}{\partial x} \Big|_{x=L} = -\frac{1}{\pi a^2} \left[ k(t)p(L,0) + \int_0^t k(t-t') \frac{\partial p(L,t')}{\partial t'} dt' \right]. \quad (26)$$

Thus the fluxes at time  $t$  are related to the densities at the end points at earlier times.

## V. CONCLUDING REMARKS

In this paper we derived an analytic expression for the spectral density of the particle number fluctuations within the channel of length  $L$ . In our theory the spectral density was obtained by Fourier transforming the survival probability of a particle initially uniformly distributed on an interval of length  $L$  with partially absorbing endpoints (where radiation boundary conditions were imposed). It follows from Eq. (2) that the spectral density at zero frequency is four times the mean lifetime of such a particle.

This lifetime can be obtained in closed form for arbitrary position-dependent diffusion coefficient  $D(x)$  and potential  $U(x)$  along the channel.<sup>21</sup> By exploiting this result we can readily obtain an analytic expression for  $S(0)$ . For example, when  $U(0)=U(L)=0$  and both  $D(x)$  and  $U(x)$  are symmetric about the center of the channel, it can be shown that

$$S(0) = \frac{\pi a}{D_b} \int_0^{L/2} e^{-\beta U(x)} dx + \frac{4 \int_0^{L/2} [e^{\beta U(x)} / D(x)] [\int_x^{L/2} e^{-\beta U(y)} dy]^2 dx}{\int_0^{L/2} e^{-\beta U(x)} dx}. \quad (27)$$

When  $D(x)=D$  and  $U(x)=0$  this reduces to  $S(0)$  in Eq. (15). Since in most experiments it is, in fact, only the zero frequency limit of the spectral density that can be readily measured, we expect that the above result will prove useful in the data analysis.

## ACKNOWLEDGMENTS

Authors thank V. Adrian Parsegian and Igor Vodyanoy for fruitful discussions. M.A.P. was also supported by the Russian State Programs on Physics of Quantum and Wave Processes (Statistical Physics Subprogram) and on Neutron Research of Matter and by RFBR Grant No. 99-02-17545.

<sup>1</sup>G. Blobel, Cold Spring Harbor Symp. Quant. Biol. **60**, 1 (1995).

<sup>2</sup>D. K. Marciano, M. Russel, and S. M. Simon, Science **284**, 1516 (1999).

<sup>3</sup>G. A. Weisman, K. D. Lustig, I. Friedberg, and L. A. Heppel, Methods in Enzymology **171**, 857 (1989).

<sup>4</sup>C. M. Feldherr, in *Nucleocytoplasmic Transport*, edited by R. Peters and M. Trendelenburg (Springer-Verlag, New York, 1986), pp. 53–61.

<sup>5</sup>B. K. Jap and P. J. Walian, Q. Rev. Biophys. **23**, 367 (1990).

<sup>6</sup>T. K. Rostovtseva and M. Colombini, Biophys. J. **72**, 1954 (1997).

<sup>7</sup>S. M. Bezrukov, J. Membr. Biol. **174**, 1 (2000).

<sup>8</sup>J. S. Bendat and A. G. Piersol, *Random Data* (Wiley, New York, 1986).

<sup>9</sup>J. M. Richardson, Bell Syst. Tech. J. **29**, 117 (1950).

<sup>10</sup>K. M. van Vliet and J. R. Fasset, in *Fluctuation Phenomena in Solids*, edited by R. E. Burgess (Academic, New York, 1965), pp. 267–354.

<sup>11</sup>R. J. van den Berg, A. de Vos, P. van den Boog, and J. de Goede, in *Noise in Physical Systems and 1/f Noise*, edited by A. D'Amico and P. Mazzetti (Elsevier, New York, 1986), pp. 213–216.

<sup>12</sup>M. W. Kim, Y. C. Chou, W. I. Goldburg, and A. Kumar, Phys. Rev. A **22**, 2138 (1980).

<sup>13</sup>G. Feher and M. Weissman, Proc. Natl. Acad. Sci. U.S.A. **70**, 870 (1973).

<sup>14</sup>H. C. Berg, *Random Walks in Biology* (Princeton University Press, New Jersey, 1993).

<sup>15</sup>T. Schirmer, T. A. Keller, Y.-F. Wang, and J. P. Rosenbusch, Science **267**, 512 (1995).

<sup>16</sup>C. Andersen, M. Jordy, and R. Benz, J. Gen. Physiol. **105**, 385 (1995).

<sup>17</sup>H. C. Berg and E. M. Purcell, Biophys. J. **20**, 193 (1977).

<sup>18</sup>S. M. Bezrukov, I. Vodyanoy, and V. A. Parsegian, Nature (London) **370**, 279 (1994).

<sup>19</sup>M. Lax and P. Mengert, Phys. Chem. Solids **14**, 248 (1960).

<sup>20</sup>R. Zwanzig and A. Szabo, Biophys. J. **60**, 671 (1991).

<sup>21</sup>A. Szabo, K. Schulten, and Z. Schulten, J. Chem. Phys. **72**, 4350 (1980).